The Development of γ-γ' Lamellar Structures in a Nickel-Base Superalloy during Elevated Temperature Mechanical Testing

REBECCA A. MacKAY and LYNN J. EBERT

Changes in the morphology of the γ' precipitate were examined during creep and tensile testing at temperatures between 927 and 1038 °C in [001]-oriented single crystals of a model Ni-Al-Mo-Ta superalloy. In this alloy, the γ' particles link together to form lamellae, or rafts, which are aligned with their broad faces perpendicular to the applied tensile axis. The dimensions of the γ and γ' phases were measured as the lamellar structure developed and were related to time and strain in an attempt to trace the changing γ-γ' morphology. The results showed that directional coarsening of γ' began during primary creep, and the attainment of a fully developed lamellar structure did not appear to be directly related to the onset of steady-state creep. The rate of directional coarsening during creep increased as the temperature was raised and also increased as the stress level was raised at a given testing temperature. The raft thickness remained equal to the initial γ' size from the start of the creep test up through the onset of tertiary creep for all testing conditions. It was found that extensive rafts did not develop during the shorter testing times of the tensile tests, and that tensile testing of pre-rafted structures did not alter the morphology of the rafts. The overall behavior of the alloy was a clear indication of the stability of the finely-spaced γ-γ' lamellar structure.

I. INTRODUCTION

NICKEL-base superalloys derive much of their superior high temperature strength from the precipitation of γ'. Changes in the cuboidal morphology of the γ' precipitates were first observed in commercial nickel-base alloys[1–5] after prolonged creep exposures. These γ' phase instabilities were viewed initially with concern, and this led to many proposals[2,6–8] suggesting the elimination of directional γ' stringers through alloy design.

However, directional coarsening of the γ' precipitate has received renewed attention.[9–19] Recent results[9,10] have demonstrated that directional coarsening significantly enhances high temperature creep properties in the [001] orientation when the γ-γ' lamellae which form during creep are continuous and finely-spaced. The lamellar structure which developed perpendicular to the applied stress provided a beneficial structure for creep resistance, because circumvention of the γ' phase by dislocation climb would be eliminated.[9,10] By preventing the dominant creep mechanism from occurring at high temperatures, significant creep deformation could proceed only by the more sluggish process of shearing of the γ' phase. It is also recognized now that the directional coarsening process is highly dependent upon the initial condition of the microstructure prior to mechanical testing. In particular, the γ' size,[13,14] as well as the degree of coherency between the precipitate and the matrix,[14] substantially influence the subsequent γ-γ' lamellar morphology and creep properties.

These results indicate that directional coarsening can exert a strong influence on the mechanical properties of nickel-base superalloys. However, the need for further understanding in this area is apparent. Investigations concerning the actual development of γ-γ' lamellae under several testing conditions would appear to be of considerable interest. Thus, the purpose of this study was to examine the kinetics of the formation and subsequent development of directional coarsening of the γ' precipitate in model nickel-base superalloy single crystals. In a previous paper,[14] the influence of initial γ' size on the microstructural development under one set of creep testing conditions was considered. In the present investigation, directional coarsening was examined during tensile creep under various stress levels at 982 and 1038 °C. Specifically, the dimensions of the γ and γ' phases were related to creep time and strain in an attempt to trace the changing γ-γ' morphology. A few crystals were also tensile tested to examine directional coarsening under more rapid strain rates.

II. MATERIAL AND EXPERIMENTAL PROCEDURES

Single crystals of a Ni-Al-Mo-Ta composition were produced by directional solidification using the withdrawal process. The 1.25 cm diameter single crystal bars were heat treated in an argon atmosphere in the following sequence: 1277 °C for four hours, 1288 °C for two hours, 1299 °C for two hours, and 1313 °C for 100 hours in order to produce chemical homogeneity. The heat treated bars then were forced-air quenched to ambient temperature. The composition of the heat treated alloy was determined by bulk wet chemistry and by microprobe to be the following (in wt pct): 5.8 Al, 14.6 Mo, 6.2 Ta, and balance Ni. This composition is similar to that studied by Pearson and co-workers.[9,10]

Test specimens with a gage diameter of 4.6 mm and a gage length of 19.0 mm were machined by precision grinding from the heat treated bars. Constant load tensile creep tests were performed in air between 927 and 1038 °C on single crystal specimens having orientations within 10 deg of [001]. Creep extensions were measured with extensometers in conjunction with linear variable differential transformers and strip chart recorders. The extensometer

REBECCA A. MacKAY is Materials Scientist with NASA Lewis Research Center, Cleveland, OH 44135. LYNN J. EBERT is Professor of Metallurgy and Materials Science, Case Western Reserve University, Cleveland, OH 44106.

Manuscript submitted March 25, 1985.

knife edges were placed in circumferential v-notches located at each end of the specimen gage length. Although some tests were run to failure, most creep tests were interrupted prior to failure at various times. Each interrupted test specimen was rapidly cooled to ambient temperature under load. Tensile tests also were performed between 927 and 1038 °C at strain rates of 1.1×10^{-4} s^{-1}.

Upon completion of testing, specimens were sectioned on a slow-speed saw along planes parallel to the applied stress axis. Specimens were prepared by standard metallographic techniques for examination by scanning electron microscopy (SEM). In order to analyze the changing microstructure in a quantitative manner, a line intercept technique was performed directly on the photomicrographs with the aid of the plotter of a computer. To obtain the γ' raft length dimension, line scans were traversed in a direction perpendicular to the stress axis. To obtain the raft thickness and the interlamellar spacing, the line scans were traversed parallel to the stress axis, and the edge-to-edge distances of the γ' and γ phases, respectively, were determined. For each tested specimen, between 150 and 250 γ' particles or rafts were measured.

III. RESULTS

A. *Creep Properties*

The homogenized and quenched Ni-Al-Mo-Ta single crystals were creep tested under several stress levels at 927, 982, and 1038 °C. The typical creep curves for the specimens exhibited stages of primary, steady-state, and tertiary creep, although the amount of primary creep was limited. The primary creep rate decreased continuously and was followed by a rather rapid transition into steady-state creep. The slope of the linear portion of the steady-state creep region was defined as the steady-state creep rate, $\dot{\varepsilon}_s$. Examples of these creep curves are shown in Figures 1(a) through (d).

The creep rupture properties were characterized in terms of the stress and temperature dependence of the steady-state creep rate, $\dot{\varepsilon}_s$, and the rupture life, t_f. The steady-state creep rate can be described by the following phenomenological equation:[20]

$$\dot{\varepsilon}_s = A\sigma^n \exp(-Q/RT) \qquad [1]$$

where A and n are constants, Q is the apparent activation energy for creep, R is the universal gas constant, and T is the creep testing temperature in °K. The linear behavior of the double logarithmic plot of steady-state creep rate *vs* applied stress is illustrated in Figure 2 for the single crystals tested at 927, 982, and 1038 °C. Based on the limited stress ranges used, the values of the slope, n, were estimated at 8.7 for 927 °C, 9.2 for 982 °C, and 10.9 for 1038 °C. However, the differences in the values of the stress exponent throughout this temperature regime were not statistically significant. Since the value of n was independent of temperature, then the apparent activation energy of creep was independent of stress. Thus, n and Q were estimated by multiple regression techniques using all of the creep data obtained at 927, 982, and 1038 °C. The coefficients, n and Q, of the regression equation were found to be equal to 10.0 ± 0.7 and 475 ± 109 kJ/mol, respectively.

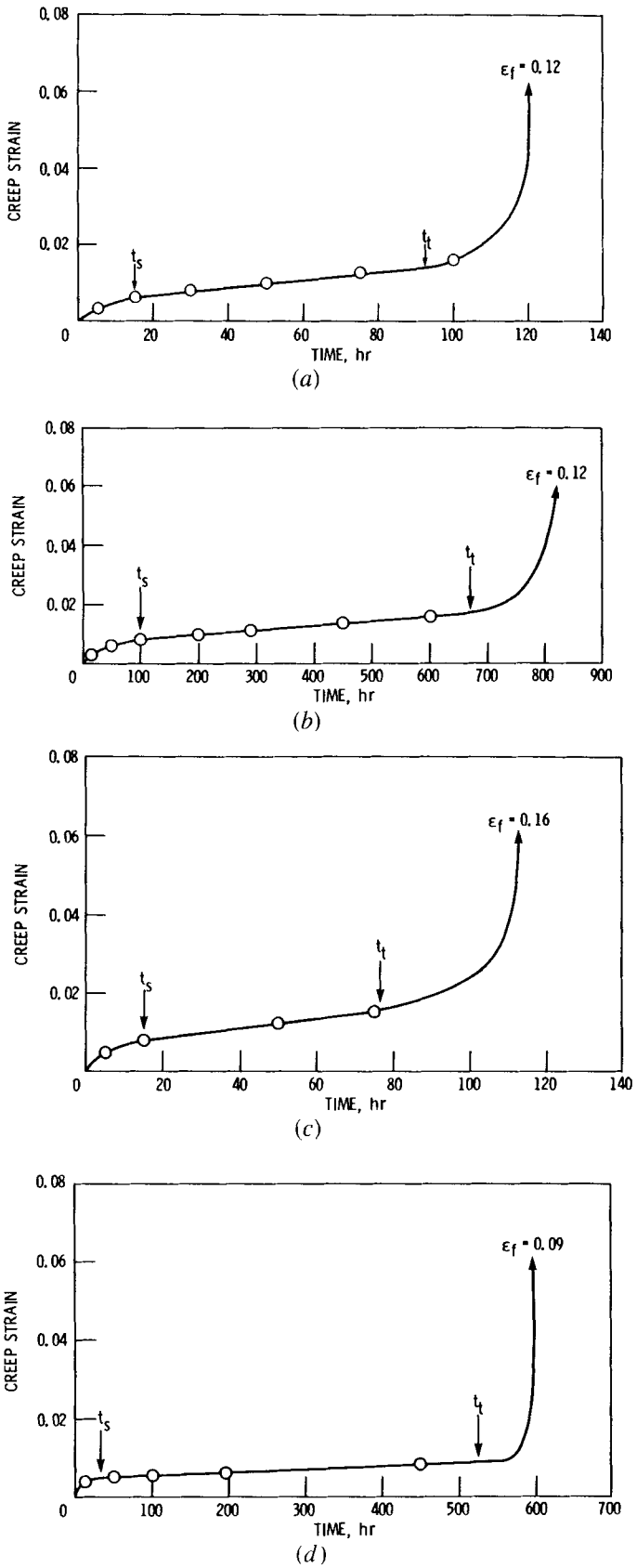

Fig. 1—Typical creep curves of the Ni-Al-Mo-Ta single crystals tested at (*a*) 982 °C and 234 MPa; (*b*) 982 °C and 186 MPa; (*c*) 1038 °C and 179 MPa; and (*d*) 1038 °C and 147 MPa. The open circles correspond to the specimens whose tests were interrupted at specific times. The times to the onset of steady-state creep, t_s, and to the onset of tertiary creep, t_t, are indicated by the arrows.

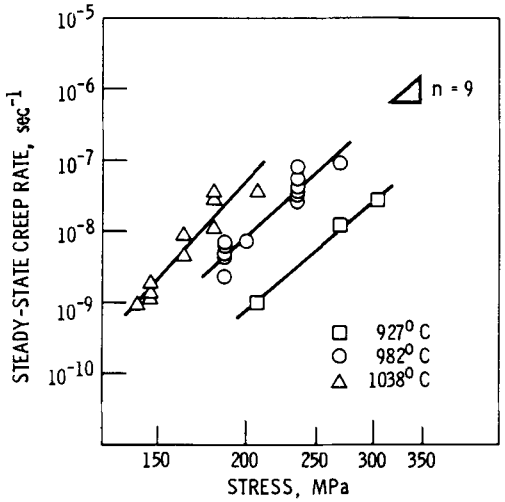

Fig. 2—The stress dependence of steady-state creep rate is illustrated at 927, 982, and 1038 °C. A slope, or stress exponent, n, of 9 is shown for comparison.

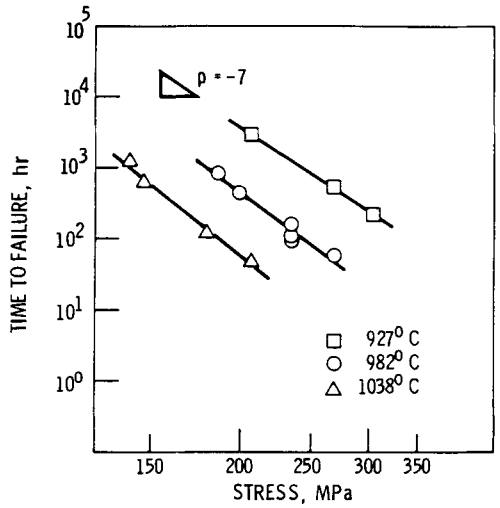

Fig. 3—The stress dependence of creep rupture life is illustrated at 927, 982, and 1038 °C. A slope equal to −7 is shown for comparison.

In addition, the stress and temperature dependence of the creep rupture lives was described accurately by the following equation:[21]

$$t_f = A\sigma^p \exp(-Q/RT) \quad [2]$$

which is of the same form as Eq. [1]. The linear behavior of the log t_f *vs* log σ data is illustrated in Figure 3 in the temperature range between 927 and 1038 °C. The values of the slopes, p, for these data were equal to −6.7 at 927 °C, −7.5 at 982 °C, and −8.1 at 1038 °C. The confidence intervals around these slopes were obtained, and it was determined that the values of p were statistically equivalent. The coefficients p and Q were determined by multiple regression and were found to be equal to -7.6 ± 0.4 and 506 ± 67 kJ/mol, respectively.

B. γ' *Shape Changes during Creep*

The homogenization treatment employed removed the elemental segregation that was present in the as-cast condition and refined the γ' dispersion in the γ matrix. Examples of the homogenized and forced-air cooled microstructure are given in Figures 4(a) and (b). The microstructure contained cuboidal γ' particles which had a mean edge length of 0.3 μm, and as evident in Figure 4(b), some misfit dislocations were present in the γ-γ' interfaces. When a uniaxial tensile stress was applied, the γ' particles linked up to form platelets which had their broad faces perpendicular to the applied stress axis. The microstructural changes which occurred during creep under several combinations of temperature and stress will be considered in detail below.

A typical creep curve of the Ni-Al-Mo-Ta single crystals tested at 982 °C and 234 MPa is depicted in Figure 1(a). The corresponding microstructures of specimens from selected interrupted tests under these conditions are shown in Figure 5. These scanning electron micrographs illustrate the development of directional coarsening of the γ' phase from a cuboidal to a plate-like morphology during creep; the stress axis is vertical in all photos. The needle-like phase present in these micrographs is the NiMo δ phase; it formed because of a supersaturation of molybdenum in this heat. The influence that this phase had on the microstructure and on the resultant creep properties has been considered previously.[14,18]

As may be seen in Figure 1(a), the crystal was in primary creep after five hours under a stress of 234 MPa at 982 °C. The corresponding microstructure in Figure 5(a) shows that some of the γ' particles had started to link together, although many were still individual cubes. The single crystal made the transition from primary into steady-state creep after 15 hours, and Figure 5(b) shows that many more particles had joined into platelets by this time. After 50 hours, the crystal was well into steady-state creep, and the γ' rafts had continued to develop under stress, as illustrated by their increased lateral extension in Figure 5(c). At this time, the rafts were about as fully developed as possible and extended completely across the area depicted in this micrograph. That is, the lamellae were continuous and interconnected throughout the specimen, and this γ' morphology did not change further with increased time of stress annealing from this point, up through the onset of tertiary creep. Although the thickness of the rafts appeared to remain constant throughout most of the creep test, the rafts in the failed condition had coarsened, as shown in Figure 5(d). The microstructures of the failed specimens are representative of those within the uniform gage section, away from the necked region. In general, the lamellar structures were significantly coarser near the fracture surface.[18]

A typical creep curve obtained for the crystals tested at 982 °C and 186 MPa is illustrated in Figure 1(b). The changes in the microstructural features under these conditions were similar to those at 982 °C and 234 MPa, although these changes occurred at a slower rate at the lower stress level. As shown in Figure 6(a), many of the γ' particles were linked together after 15 hours of testing at 982 °C and 186 MPa. The γ' rafts became more extensive laterally with increased time of stress annealing through the primary creep region. It is discernible in Figure 6(b) that the specimen

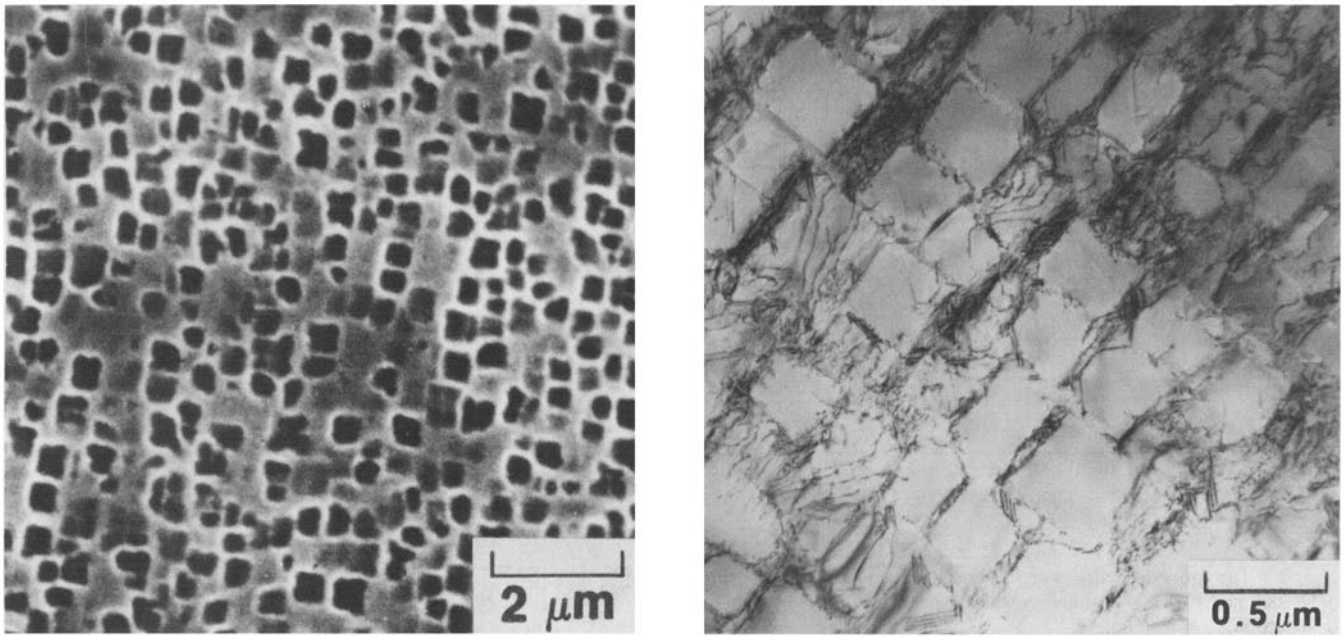

(*a*) (*b*)

Fig. 4—Refined γ' dispersion produced by homogenization and forced-air quenching to ambient temperature: (*a*) SEM photo; and (*b*) TEM photo showing some misfit dislocations at the γ-γ' interfaces.

had continuous and interconnected rafts after 199 hours of testing. Comparison of Figures 6(b) through (d) indicates that the rafts did not appear to thicken with time, even in the failed condition. Envelopes of γ' did develop around needles of δ phase as the creep time increased. These localized areas were avoided when comparisons of the raft dimensions were made.

A creep curve of the Ni-Al-Mo-Ta single crystals tested at 1038 °C and 179 MPa is presented in Figure 1(c). This combination of temperature and stress produced essentially the same creep rate and rupture life as those which resulted from the tests at 982 °C and 234 MPa. As illustrated in Figure 1(c), the single crystal was in primary creep after five hours under stress. The corresponding microstructure in Figure 7(a) shows that most of the cuboids had started to link together, although vertical bridges of γ which separated the γ' particles were still present. The crystal made the transition into steady-state creep after 15 hours. The micrographs in Figures 7(b) and (c) indicate that the rafts became more extensive in the lateral direction after the onset of steady-state creep. As may be seen in Figure 7(c), most of the rafts extended completely across the micrograph after 50 hours. This γ' morphology did not change further with increased time of creep testing, at least up to the onset of tertiary creep. However, as evident in Figure 7(d), the lamellae in the failed specimen had become more coarsely spaced.

Finally, the typical creep curve obtained for the crystals at 1038 °C and 147 MPa is shown in Figure 1(d); the corresponding SEM micrographs of the specimens tested under these conditions are given in Figure 8. The γ' cuboids started to link together within the first fifteen hours, as shown in Figure 8(a), and the γ' rafts continued to develop in the lateral direction up to 100 hours of creep testing. The transition into steady-state creep was obtained after about 35 hours of testing. Comparison of Figures 8(b) through (d) shows that little change is discernible in the microstructure from that after 100 hours of testing to that in the failed condition.

C. *Quantitative Metallography*

In order to quantify the changing microstructure during creep at 982 and 1038 °C, measurements of γ' raft length, γ' raft thickness, and interlamellar, or γ, spacing were obtained from the SEM photos. The mean raft dimensions are plotted as a function of time in Figures 9 through 12 for each creep testing condition. The lines delineated in these figures were determined by standard least squares regression techniques. The times to the onset of steady-state creep, t_s, and to the onset of tertiary creep, t_t, also are indicated in these figures for comparison to the creep curves. The γ' volume fraction remained constant at approximately 60 pct throughout the creep tests in this temperature regime.

Figure 9 illustrates that the mean raft length increased linearly with time up to almost 50 hours of creep testing at 982 °C and 234 MPa. After 50 hours, the crystal was well into steady-state creep, and the values of the raft lengths reached a plateau and remained constant thereafter. This plateau occurred when directional coarsening was complete and the microstructure consisted of continuous, interconnected γ' lamellae, such as those depicted in Figure 5(c). In contrast to the raft length, the mean raft thickness remained constant at about 0.33 μm up through the onset of tertiary creep. Linear regression indicated that the slope through these data points was not statistically different from zero. However, the single crystals in the failed condition had undergone a substantial increase in the total amount

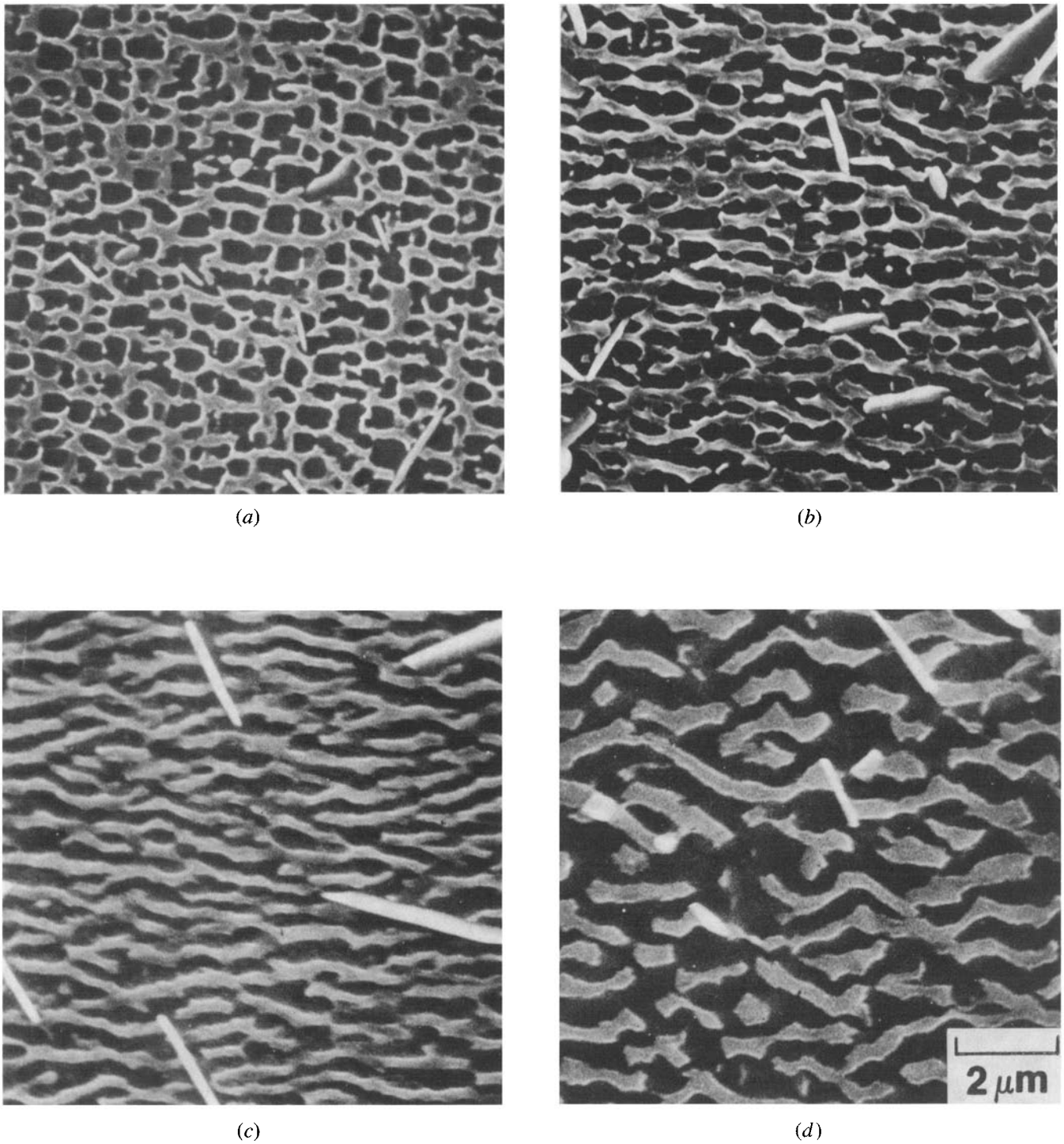

Fig. 5 — The development of directional coarsening of γ' at 982 °C and 234 MPa is illustrated at: (*a*) 5, (*b*) 15, (*c*) 50, and (*d*) 120 hours, in failed condition. The stress axis is vertical in all photos.

of strain during tertiary creep, and the rafts in the failed condition had coarsened considerably. As may be noted in Figure 9, this increase in thickness was abrupt, because the specimen whose test was interrupted after the onset of tertiary creep showed no increase in raft thickness. The interlamellar spacing, or thickness of the γ phase, also is plotted as a function of time in Figure 9, and these data displayed the same general behavior as the raft thickness *vs* time data. The mean raft dimensions for the specimens tested at 982 °C and 186 MPa are plotted *vs* time in Figure 10. The raft length increased linearly with time during first-stage creep, and these values stabilized at approximately 1 μm near the onset of steady-state creep. Both the raft thickness and interlamellar spacing remained constant throughout this creep curve, even in the failed condition.

Figure 11 displays the mean raft dimensions as a function of time for the specimens tested at 1038 °C and 179 MPa. The raft length increased linearly with time up to about the

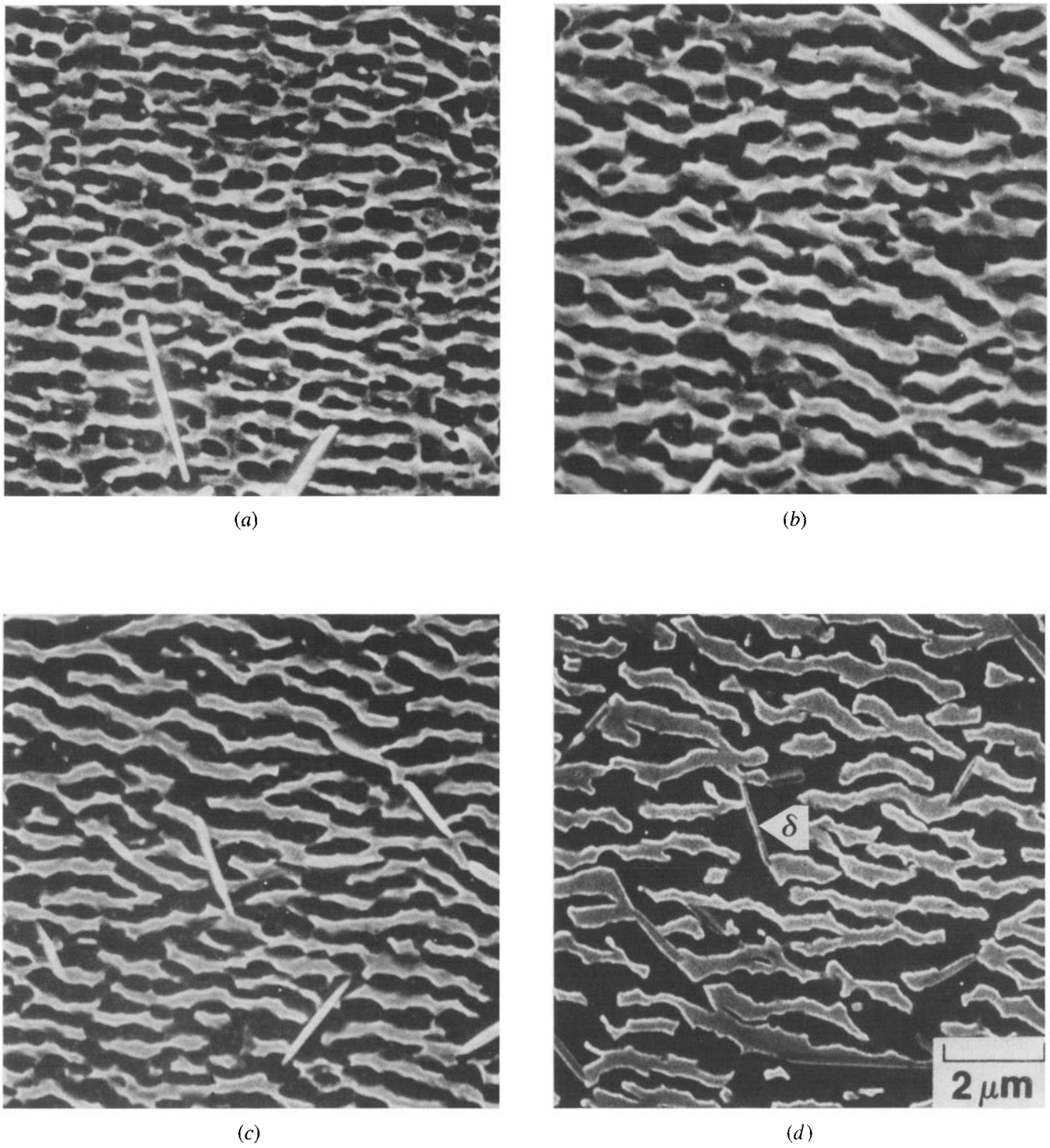

Fig. 6—The development of directional coarsening of γ' at 982 °C and 186 MPa is illustrated at: (*a*) 15, (*b*) 199, (*c*) 450, and (*d*) 831 hours, in failed condition. The stress axis is vertical in all photos.

onset of steady-state creep, and a plateau region was attained in mean raft length shortly thereafter. Both the thickness and interlamellar spacings were constant from the start of the test up through the onset of tertiary creep; however, in the failed condition, a substantial increase in these dimensions was measured. The directional coarsening behavior exhibited under these conditions was very similar to that at 982 °C and 234 MPa. Finally, the mean raft dimensions of the specimens creep tested at 1038 °C and 141 MPa are plotted as a function of time in Figure 12. The raft length continued to increase with time past the onset of steady-state creep, but by 100 hours, the raft length had stabilized at a constant value. The raft thickness and interlamellar spacing both remained constant throughout the creep test, even in the failed condition.

The γ' rafting rates measured at 982 and 1038 °C are plotted against the applied stress levels in Figure 13. These rafting rates were determined by the positive slopes of

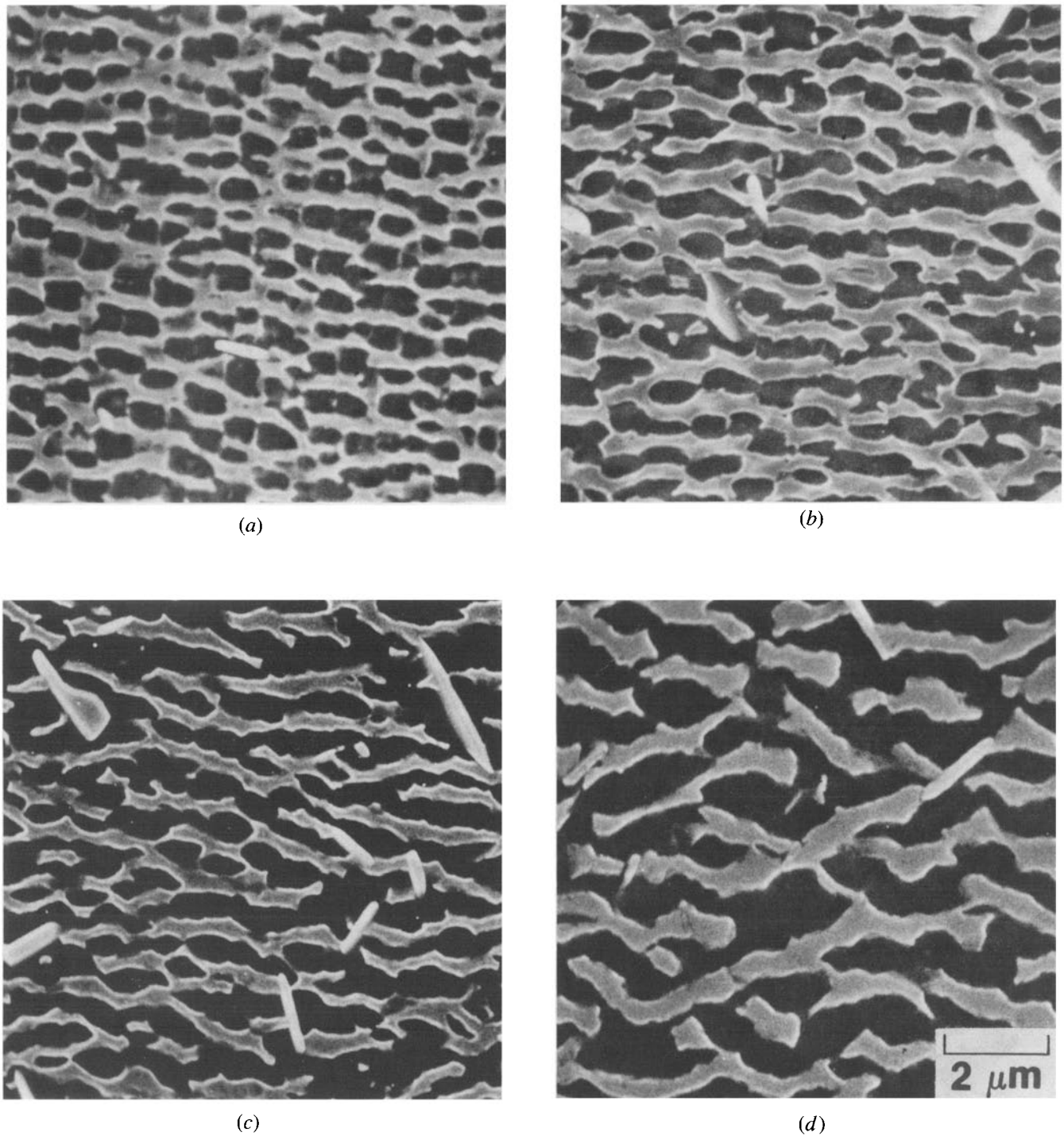

Fig. 7—The development of directional coarsening of γ' at 1038 °C and 179 MPa is illustrated at: (*a*) 5, (*b*) 15, (*c*) 50, and (*d*) 116.3 hours, in failed condition. The stress axis is vertical in all photos.

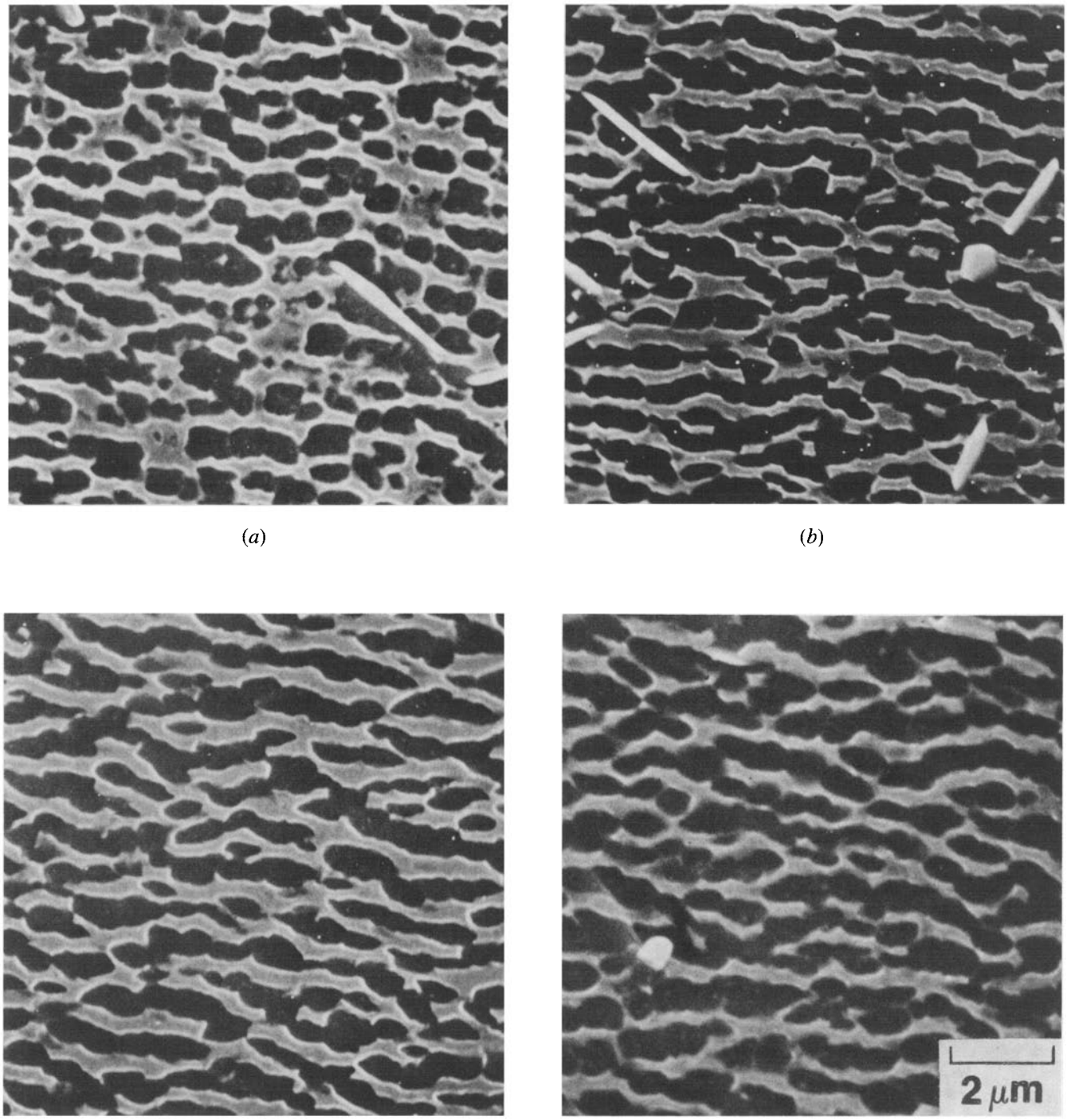

Fig. 8—The development of directional coarsening of γ' at 1038 °C and 147 MPa is illustrated at: (*a*) 15, (*b*) 100, (*c*) 195, and (*d*) 598 hours, in failed condition. The stress axis is vertical in all photos.

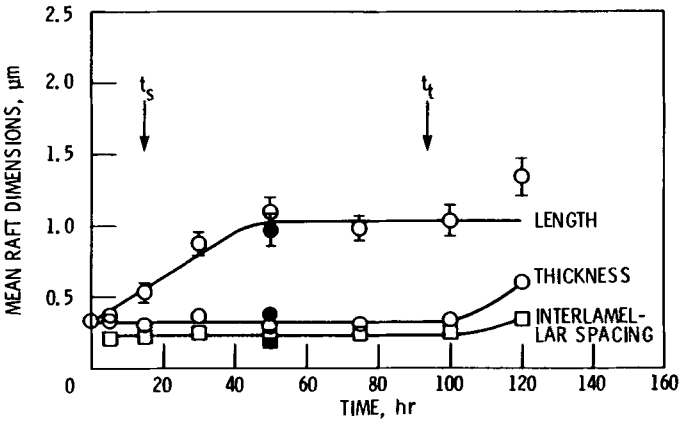

Fig. 9—The mean dimensions of the γ' rafts are plotted as a function of time during creep at 982 °C and 234 MPa. Error bars for 95 pct confidence intervals were drawn when end points of intervals were outside of data point symbols. Solid symbols indicate raft dimensions for the pre-rafted plus tensile tested specimens.

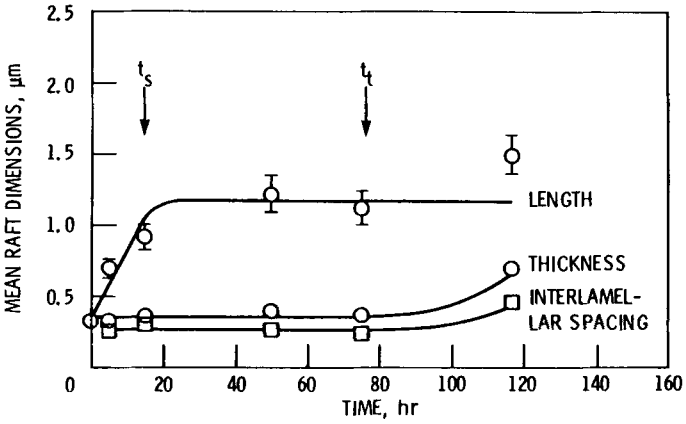

Fig. 11—The mean dimensions of the γ' rafts are plotted as a function of time during creep at 1038 °C and 179 MPa. Error bars for 95 pct confidence intervals were drawn when end points of intervals were outside of data point symbols.

the mean raft length *vs* time data, shown previously in Figures 9 through 12. It may be seen in Figure 13 that the rafting rate increased as the stress level was raised at a given testing temperature. Specifically, when the stress level at 982 °C was increased from 186 to 234 MPa, the rafting rate increased by a factor of 1.5. At 1038 °C, the rafting kinetics were nearly four times more rapid at 179 MPa than at 147 MPa. As a result, the fully developed lamellae, which are representative of the plateau region, formed sooner for the specimens at the higher stress levels.

Figure 13 also indicates that the rafting rate increased as the temperature was raised from 982 °C to 1038 °C, over the range of stress levels utilized in the present study. Comparison of the rafting data for specimens tested at the highest stress levels at 982 and 1038 °C shows that the kinetics of rafting at 1038 °C were about three times faster than those at 982 °C. These two conditions of temperature and stress produced equivalent creep lives of about 120 hours, as well as equivalent steady-state creep rates. Thus, this increase of 56 °C produced a three-fold increase in rafting rate for equal deformation rates. Temperature seemed to have less of an effect on the rafting kinetics at the lower stresses, as is evident in Figure 13. Since the slopes of the data in Figure 13 differed for each temperature, the apparent activation energy for rafting was estimated at a specific stress level, 179 MPa, using an Arrhenius relation analogous to that in Eq. [1]. The activation energy for rafting at 179 MPa was found to be approximately 380 kJ/mol.

The relationship between the mean raft length and creep strain for the specimens tested at 982 °C is presented in Figure 14. The lines in the figure were drawn using the predicted raft length values obtained from linear regression of the data in Figures 9 and 10 and from the values of creep strain in Figures 1(a) and (b). Figure 14 shows that the raft length increased with increasing creep strain up to a plateau; however, these data did not follow a linear relationship as did the raft length *vs* time data. Instead, the curvature in Figure 14 was related to the continually decreasing creep

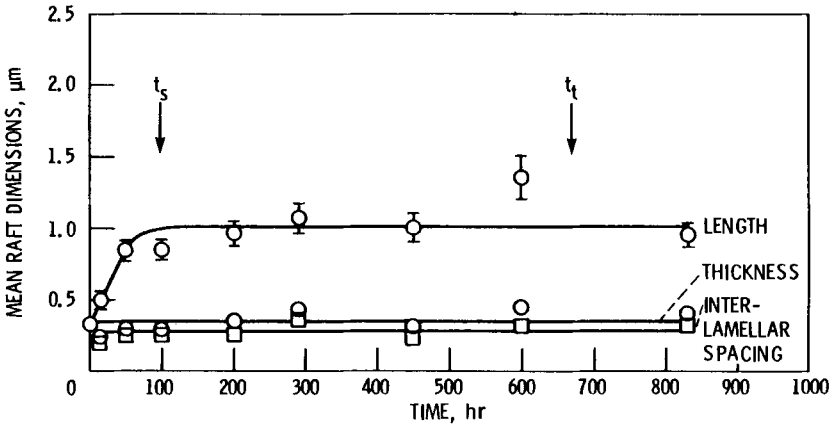

Fig. 10—The mean dimensions of the γ' rafts are plotted as a function of time during creep at 982 °C and 186 MPa. Error bars for 95 pct confidence intervals were drawn when end points of intervals were outside of data point symbols.

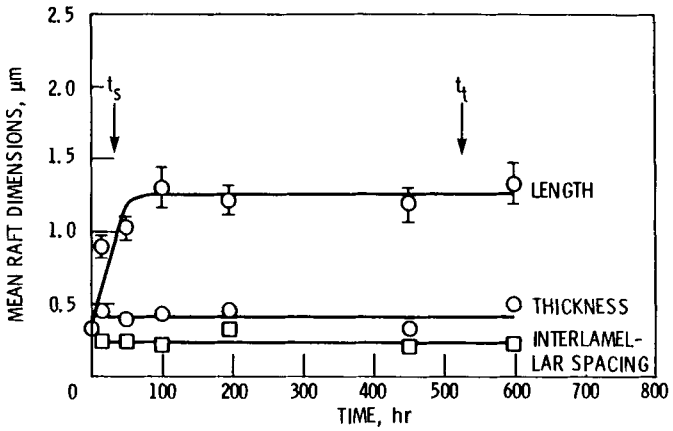

Fig. 12—The mean dimensions of the γ' rafts are plotted as a function of time during creep at 1038 °C and 147 MPa. Error bars for 95 pct confidence intervals were drawn when end points of intervals were outside of data point symbols.

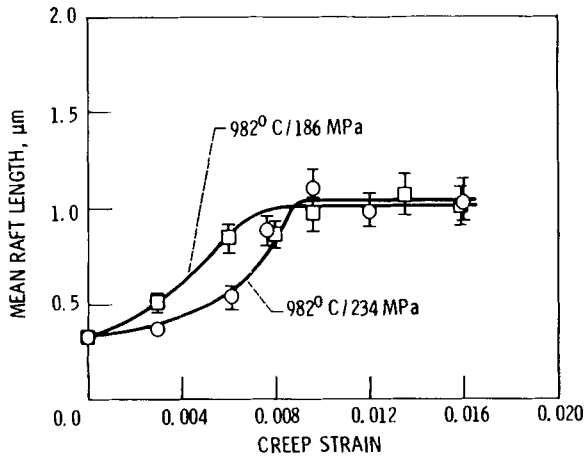

Fig. 14—The relationship between mean raft length and creep strain is illustrated for the specimens tested at 982 °C.

rate in the primary creep stage. When the rafts were fully formed, a plateau in raft length occurred at a creep strain which was slightly less than 1 pct. A similar relationship between raft length and creep strain was exhibited by the specimens tested at 1038 °C.

D. *Tensile Properties*

Tensile tests were performed on the single crystals at 927, 982, and 1038 °C. The values of ultimate tensile strength (UTS) and 0.2 pct yield strength (YS) are plotted as a function of temperature in Figure 15. The UTS and YS of the as-solutioned specimens decreased in a similar manner as the testing temperature was increased. The microstructures of failed specimens after tensile testing at 982 and 1038 °C are shown in Figures 16(a) and (b), respectively. It is apparent in Figure 16(a) that many of the γ' particles were still separated by vertical bridges of γ after tensile testing at 982 °C. Directional coarsening was more developed after tensile testing at 1038 °C, as evident in Figure 16(b), although the γ' platelets were discrete and did not extend completely across the micrograph.

An experiment was performed to determine if accumulated strain would be sufficient to cause thickening of the γ' plates, similar to that which was observed after tertiary creep at the higher stress levels. However, it was desired to allow deformation to occur without allowing much time for diffusion to occur simultaneously. To accomplish this, a specimen was first creep tested at 982 °C and 234 MPa; this test was interrupted after 50 hours of creep, so that the microstructure of the specimen consisted of fully developed and finely-spaced rafts, similar to that in Figure 5(c). The raft dimensions of this specimen corresponded to those within the plateau region in mean raft length in Figure 9. This pre-rafted specimen was then tensile tested to failure at

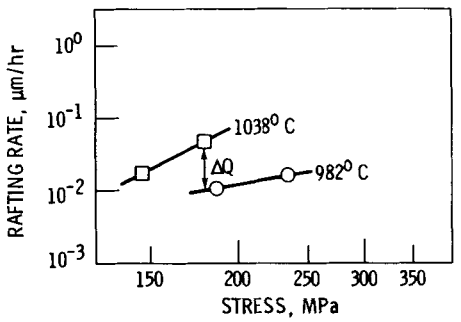

Fig. 13—The stress dependence of the rafting rate is illustrated at 982 and 1038 °C. The stress at which the apparent activation energy, Q, for rafting was measured is also indicated.

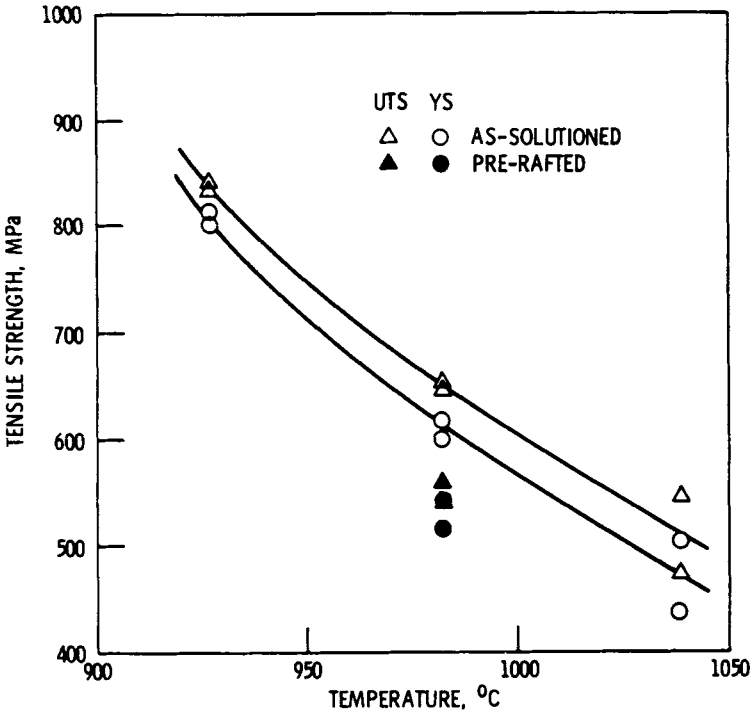

Fig. 15—The ultimate tensile strength (UTS) and 0.2 pct yield strength (YS) are illustrated as a function of temperature. Open symbols correspond to specimens in the as-solutioned condition. Closed symbols correspond to specimens which were pre-rafted prior to tensile testing.

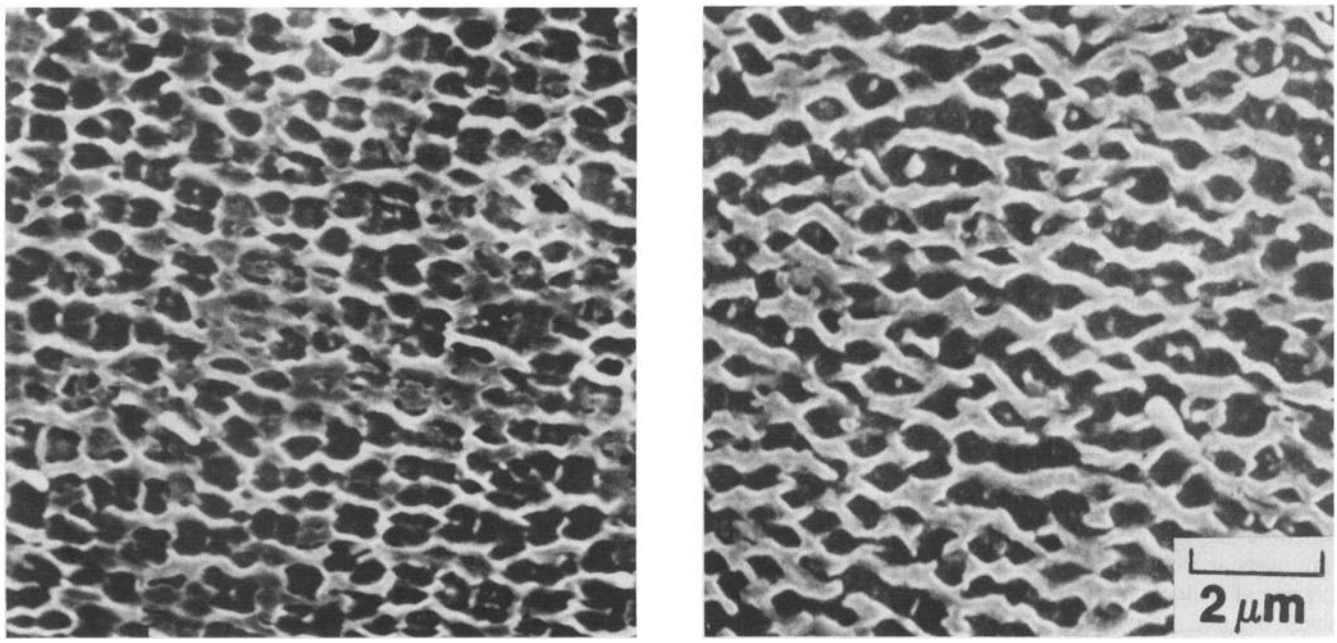

(*a*) (*b*)

Fig. 16—γ-γ' microstructures in failed specimens after tensile testing at (*a*) 982 and (*b*) 1038 °C.

the same temperature, 982 °C. As shown in Figure 15, these pre-rafted specimens exhibited a lower UTS and YS than the as-solutioned specimens tensile tested at 982 °C. The pre-rafted specimens had a slightly lower total elongation, 12.2 pct, as compared to about 17.2 pct for the as-solutioned specimens. The dimensions of the γ and γ' phases of the pre-rafted plus tensile tested specimens were measured and are indicated by the solid symbols in Figure 9. Comparison of the data in this figure shows that the raft dimensions after pre-rafting for 50 hours of creep, plus tensile testing to failure, were essentially the same as those after 50 hours of creep for the as-solutioned specimens.

IV. DISCUSSION

A. *Creep Properties*

The similarities of the stress dependent creep data in Figures 2 and 3 imply that the same factors are controlling creep deformation between 927 and 1038 °C. The creep behavior of this model superalloy is similar to that in other superalloys in which values of $n > 5$ and Q values greater than the activation energy for self-diffusion are frequently observed.[19,22–24] In addition, the activation energy for rafting was found to be reasonably close to that for creep, given the limited data used to determine the activation energy for rafting. These estimates suggest that similar factors were controlling both processes. However, a more complete understanding of the relationship between creep, directional coarsening, and diffusion would require a consideration of the temperature dependencies of other factors such as elastic moduli, lattice mismatch, and γ' volume fraction.

B. *Raft Lengthening*

It is clear from examination of Figures 9 through 12 that the γ' rafting development was very similar in all of the testing conditions studied. Directional coarsening began during primary creep, and the raft lengths increased with time in a linear fashion. Faster rafting rates were obtained at more elevated temperatures because of more rapid diffusion rates at these higher temperatures. Higher stress levels also increased the kinetics for rafting by hastening the stress-assisted diffusion process. When rafting kinetics were increased, directional coarsening was completed in less time, and the plateau in mean raft length was observed earlier. In this alloy, raft development was generally completed within the first 20 pct of the creep life of the specimen.

The rapid development of directional coarsening in the present alloy is contrary to the observations made in other superalloys, in which the agglomeration of γ' proceeded slowly during steady-state creep;[24,25] this morphological change was considered to initiate the onset of tertiary creep. However, rapid directional coarsening now appears to be more common than previously thought, as the rafting rates exhibited in the present alloy seem comparable to the microstructural observations in other alloys, such as NASAIR 100,[11,15,19] CMSX-2,[13]* and IN 713.[16,26]**

*CMSX-2 is a registered trademark of Cannon-Muskegon Corporation.
**IN 713 is a registered trademark of the INCO family of alloys.

A simple mechanism for the development of directional coarsening can be envisioned as follows. The γ'-forming species flow toward the vertical faces of unlinked γ' particles; and the γ-forming species that are present in the vertical bridges, which initially separate the γ' particles, diffuse in the opposite direction. It appears that the matrix and precipitate-forming species must be flowing in opposite directions simultaneously, because directional coarsening progresses rapidly under small amounts of creep strain. Furthermore, a competitive growth situation, similar to that in Ostwald ripening, is suggested to occur during this process, whereby the small γ' particles dissolve at the expense of the larger particles which increase in length. The introduction of an applied stress may also cause the dissolution of γ' particles which are unfavorably positioned with respect to nearby platelets that have started to develop. This selection of

favorably located particles for growth has also been rationalized for zero-stress aging behavior in Ni-Al alloys.[27] As the platelets lengthen, the total number of discrete precipitates in the system decreases, and thus the γ' volume fraction remains constant during the process.

Under some of the testing conditions employed in the present study, the raft length did continue to increase after the transition was made into steady-state creep. This observation seems to support the idea that directional coarsening development is related to both accumulated strain and time. As suggested elsewhere,[28] there may be limitations to the applicability of purely elastic considerations in the interpretation of morphological changes of the γ' precipitate during stress coarsening. Furthermore, it appears that the formation of fully developed rafts was not directly related to the onset of second-stage creep. Apparently, sufficient strain hardening for the transition into steady-state creep was obtained by the material prior to the onset of the plateau in mean raft length, perhaps through the interaction of interfacial dislocations with mobile dislocations as the γ' platelets linked together.

Once the directional coarsening process was completed, however, measurements of the γ' raft length remained at a constant value. This plateau in mean raft length signified that a change in the microstructure had occurred. Before the plateau was attained, the microstructure consisted of discrete particles or small platelets of γ' within the matrix. However, after the onset of the plateau, the microstructure consisted of continuous, interpenetrating lamellae of γ and γ'. These rafts extended over large distances across the specimen diameter and were interrupted only by an occasional sub-boundary, or more locally, by needles of δ phase.

C. *Raft Thickening*

The thickness of the rafts was found to be equal to the γ' size which was present prior to testing; this dimension remained at this initial value, up through at least the onset of tertiary creep. Measurements of the interlamellar spacing followed the same behavior as the raft thickness data. This behavior was an indication of the stability of the finely-spaced rafted structure. However, in the failed condition for the specimens tested at the higher stress levels at 982 and 1038 °C, the rafts had thickened considerably. It appears that thickening may be enhanced by the substantial amount of total strain accumulated during the tertiary creep stage, since no increase in raft thickness was observed at, or shortly after, the onset of tertiary creep. A mechanism of γ' raft thickening is suggested here, whereby γ' shearing causes the formation of small ledges at the γ-γ' interfaces. These ledges can enhance thickening of precipitate plates,[2,29] given sufficient time for diffusion. As lamellar thickening proceeds, the number of γ-γ' interfaces would be reduced, since the γ' volume fraction remains constant during creep. This would increase the creep rate, and in turn, would produce more shearing and additional plate thickening, such that an autocatalytic process would develop.[2] Further support for this thickening mechanism was provided by the coarser lamellae which developed in the necked regions during tertiary creep.[18] The specimens which were tested under the lower stress levels at 982 and 1038 °C, however, did not exhibit an increase in raft thickness in the failed condition. The difference in thickening behavior between specimens tested under different stress levels at the same temperature is somewhat puzzling, since all the specimens underwent similar amounts of total deformation after failure.

The γ-γ' lamellae after pre-rafting plus tensile testing at 982 °C were the same as those in the pre-rafted condition prior to tensile testing. It appears that although a large amount of strain caused lamellar thickening in 20 hours of tertiary creep at 982 °C and 234 MPa, thickening did not result after the same amount of strain was produced during tensile tests which lasted only 0.3 hours. Thus, the finely-spaced rafted structure is stable, and accumulated strain plus time seem to be necessary in order to alter it.

The stability of the microstructure in the present alloy is in direct contrast to the large increases in interparticle spacing, which were believed to cause the onset of tertiary creep and failure in a number of nickel-base alloys[4,30] where directional coarsening occurred at a slow rate. In the NASAIR 100 alloy,[11,19] which underwent rapid directional coarsening, a gradual thickening of the rafted lamellae did occur after long exposures during steady-state creep. This morphological change was also reported to result in the onset of tertiary creep and failure. The resistance to raft thickening in the present alloy may be related in part to its high lattice mismatch. A large mismatch would reduce the distance between parallel misfit dislocations at the γ-γ' interfaces, thereby providing a more effective impedance to the penetration of the γ' phase by mobile dislocations. More effective barriers would delay appreciable γ' shearing and raft thickening. The composition of the alloy could also be contributing to the stability of the rafts by reducing diffusion rates due to the high level of refractory elements. The matrix of the present alloy was saturated with Mo; this could have a tendency to increase the dislocation drag stress, thereby slowing mobile dislocation motion,[10] γ' shearing, and plate thickening.

D. *Raft Measurement Technique*

Linear intercept methods have been used successfully in the determination of edge-to-edge distances within lamellar structures such as pearlite.[31] Thus, this technique seemed appropriate, particularly for measurements of the raft thickness and interlamellar spacings. However, one of the difficulties experienced in attempting to quantify the phase dimensions was that the γ-γ' system itself was changing during creep, from discrete particles in a matrix to continuous lamellae of γ and γ'. As a result, when γ' was present as discrete particles or platelets, the "interlamellar spacing" measurement did include vertical bridges of γ, as well as horizontal γ spacings. In the fully rafted structure, vertical γ bridges were not present, and thus a truer measurement of interlamellar spacing was obtained.

The measuring technique was further limited by irregularities which existed in the microstructure. One feature which caused slight difficulty was the somewhat irregular lamellae which developed; generally the platelets were not perfectly parallel to one another, but instead exhibited some waviness. So, although the lamellae in the plateau region were completely formed and extended across the specimen diameter, a maximum intercept length of only ~ 1 μm was obtained. However, the significant aspect of the plateau was not its magnitude, but rather that its onset indicated that the

lamellar structure was fully developed. A similar plateau in γ' raft aspect ratio was also measured in IN 713C[16] by a point counting method.

A higher raft length intercept was measured in the failed specimens which were tested at the higher stress levels at 982 and 1038 °C; these specimens also exhibited a substantial increase in raft thickness during tertiary creep. However, no increase in raft thickness was observed for the specimens tested at the lower stress levels at these same temperatures, and correspondingly no increase in raft length was measured in the failed condition for these specimens. This correlation suggests that an increase in raft length measured in the failed condition was related to an increase in raft thickness. Considerably thickened plates in the failed condition would allow a longer intercept length to be measured because of the waviness of the lamellae. Although the linear intercept technique did have some limitations, the results were reproducible and internally consistent, as changes in the measured dimensions corresponded to observed changes in microstructural features.

E. *Tensile Behavior*

Tensile properties were determined in order to characterize the Ni-Al-Mo-Ta alloy more fully and to see if directional coarsening would occur under more rapid strain rates. The specimens which had been run to failure during creep testing and during tensile testing in the present study underwent similar amounts of total elongation. However, in contrast to the creep tested specimens, extensive directional coarsening did not develop in the tensile tested specimens. Since the tensile tests were completed after only 0.3 hours at the strain rates utilized, it was apparent that directional coarsening did not develop because there was not sufficient time for diffusion to occur. This lends further support to the idea that strain plus time are necessary to form continuous γ-γ' lamellae.

Finally, it has been suggested[9,10] that γ' rafting improves the creep properties by preventing dislocation climb, which is the dominant deformation mechanism in nickel-base superalloys at low strain rates and elevated temperatures.[24,32,33] However, shearing of the γ' phase predominates under tensile testing conditions of high strain rates and elevated temperatures.[33,34] As shown in Figure 15, the pre-rafted specimens had lower values of UTS and YS compared to those of the as-solutioned specimens which had cuboidal γ' morphologies. It appears that the as-solutioned specimens may have had higher tensile strengths because the γ' particles remained discrete, and as a result, the microstructure contained a larger number of γ-γ' interfaces. If particle shearing was the operative deformation mode, more interfaces would be intersected by mobile dislocations along {111} planes in the as-solutioned material, since interfaces parallel to the applied stress were not present in the lamellar structure of the pre-rafted material.

These results are in contrast to those of a previous study on UDIMET* 700,[35] in which the yield strengths above 760 °C were found to be essentially independent of precipitate morphology. The reasons for these observed differences are not clear at this time, but the lower γ' volume fraction and the less extensive γ' plates which developed after stress annealing in UDIMET 700 may be contributing factors. However, the results of the present study seem consistent with the behavior of a high γ' fraction alloy which was pre-rafted and subsequently creep tested at lower temperatures[19] where γ' shearing was also thought to be operative. Thus, it is possible that directionally coarsened structures may not be beneficial if particle shearing is normally the dominant deformation mechanism.

*UDIMET is a trademark of Special Metals Corporation.

V. CONCLUDING REMARKS

Directional coarsening of the γ' particles began in this model superalloy during primary creep at temperatures between 982 and 1038 °C. The length of the γ' rafts increased linearly with time up to a plateau, which under certain conditions was reached after the onset of steady-state creep. The onset of the plateau indicated that directional coarsening was completed, and the microstructure then consisted of continuous, interpenetrating lamellae of γ and γ'. The kinetics of the directional coarsening process were increased up to a factor of four by increasing the temperature or stress level, which served to hasten stress-assisted diffusion.

The thickness of the rafts which formed was equal to the γ' size which was present prior to testing. The raft thickness remained constant at this initial value up through at least the onset of tertiary creep. The interlamellar spacing followed a similar behavior as a function of time. This was a clear indication of the stability of this continuous and finely-spaced directionally coarsened structure. Accumulated strain plus time were necessary to alter the fine γ-γ' lamellae, since tensile testing of pre-rafted specimens did not coarsen the microstructure.

Extensive directional coarsening did not develop in the single crystals during elevated temperature tensile testing, because there was not sufficient time for diffusion. It was found, however, that pre-rafted specimens had lower tensile strengths than those of as-solutioned specimens which had cuboidal γ' morphologies. It appears that rafted γ' structures are beneficial when dislocation climb is normally the operative deformation mode, such as during elevated temperature creep. Directionally coarsened structures may not be beneficial if γ' shearing is normally the dominant mechanism, since γ-γ' interfaces parallel to the stress axis are essentially eliminated.

ACKNOWLEDGMENTS

The authors wish to express their appreciation to The National Aeronautics and Space Administration for funding this work in part under NASA grant NSG-3246; Dr. C. S. Kortovich of TRW, Inc., for providing the single crystal material; and Dr. M. V. Nathal of the Lewis Research Center and Dr. D. D. Pearson of the United Technologies Research Center for many valuable discussions throughout the course of the work.

REFERENCES

1. J. R. Mihalisin and D. L. Pasquine: in *Proc. Int'l Symp. on Structural Stability in Superalloys*, Seven Springs, PA, 1968, vol. I, p. 131.
2. R. G. Davies and T. L. Johnston: in *Proc. Third Landing Conf. on Ordered Alloys*, B. H. Kear, *et al.*, eds., Claitor's Publishing Division, Baton Rouge, LA, 1970, p. 447.

3. G. A. Webster and C. P. Sullivan: *J. Inst. Metals*, 1967, vol. 95, pp. 138-42.
4. C. P. Sullivan, G. A. Webster, and B. J. Piearcey: *J. Inst. Metals*, 1968, vol. 96, pp. 274-81.
5. W. Danesi and M. Donachie: *J. Inst. Metals*, 1969, vol. 97, pp. 107-11.
6. I. L. Mirkin and O. D. Kancheev: *Met. Sci. Heat Treatment*, 1967, vol. 1, pp. 10-13.
7. J. K. Tien and S. M. Copley: *Metall. Trans.*, 1971, vol. 2, pp. 215-19.
8. J. K. Tien and S. M. Copley: *Metall. Trans.*, 1971, vol. 2, pp. 543-53.
9. D. D. Pearson, F. D. Lemkey, and B. H. Kear: in *Proc. Fourth Int'l. Symp. on Superalloys*, J. K. Tien *et al.*, eds., ASM, Metals Park, OH, 1980, p. 513.
10. D. D. Pearson, B. H. Kear, and F. D. Lemkey: in *Creep and Fracture of Engineering Materials and Structures*, B. Wilshire and D. R. J. Owens, eds., Pineridge Press Ltd., Swansea, U.K., 1981, p. 213.
11. M. V. Nathal and L. J. Ebert: *Scripta Met.*, 1983, vol. 17, pp. 1151-54.
12. R. A. MacKay and L. J. Ebert: *Scripta Met.*, 1983, vol. 17, pp. 1217-22.
13. P. Caron and T. Khan: *Mat. Sci. Eng.*, 1983, vol. 61, pp. 173-84.
14. R. A. MacKay and L. J. Ebert: in *Proc. Fifth Int'l. Symp. on Superalloys*, M. Gell *et al.*, eds., AIME, New York, NY, 1984, p. 135.
15. M. V. Nathal and L. J. Ebert: *Proc. Fifth Int'l. Symp. on Superalloys*, M. Gell *et al.*, eds., AIME, New York, NY, 1984, p. 125.
16. J. Ohe and S. Wakita: *Proc. Fifth Int'l. Symp. on Superalloys*, M. Gell *et al.*, eds., AIME, New York, NY, 1984, p. 93.
17. A. Fredholm and J. L. Strudel: *Proc. Fifth Int'l. Symp. on Superalloys*, M. Gell *et al.*, eds., AIME, New York, NY, 1984, p. 211.
18. R. A. MacKay: Ph.D. Thesis, Case Western Reserve University, Cleveland, OH, April 1984; NASA TM-83698.
19. M. V. Nathal and L. J. Ebert: *Metall. Trans. A*, 1985, vol. 16A, pp. 427-40.
20. A. K. Mukherjee, J. E. Bird, and J. E. Dorn: *Trans. ASM*, 1969, vol. 62, pp. 155-79.
21. F. Garofalo: in *Fundamentals of Creep and Creep-Rupture in Metals*, The Macmillan Company, New York, NY, 1965, p. 210.
22. J. P. Dennison, P. D. Holmes, and B. Wilshire: *Mat. Sci. Eng.*, 1978, vol. 33, pp. 35-47.
23. G. A. Webster and B. J. Piearcey: *Met. Sci. J.*, 1967, vol. 1, pp. 97-104.
24. C. Carry and J. L. Strudel: *Acta Metall.*, 1978, vol. 26, pp. 859-70.
25. C. Carry and J. L. Strudel: in *Proc. Fourth Int'l. Conf. on the Strength of Metals and Alloys*, Laboratoire de Physique du Solide, ed., Nancy, France, vol. 1, 1976, p. 324.
26. D. Schwahn, W. Kesternich, and H. Schuster: *Metall. Trans. A*, 1981, vol. 12A, pp. 155-65.
27. A. J. Ardell, R. B. Nicholson, and J. D. Eshelby: *Acta Metall.*, 1966, vol. 14, pp. 1295-309.
28. A. Pineau: *Acta Metall.*, 1976, vol. 24, pp. 559-64.
29. H. I. Aaronson, J. K. Lee, and K. C. Russell: in *Precipitation Processes in Solids*, K. C. Russell and H. I. Aaronson, eds., TMS-AIME, New York, NY, 1978, p. 31.
30. H. Burt, J. P. Dennison, I. C. Elliot, and B. Wilshire: *Mat. Sci. Eng.*, 1982, vol. 53, pp. 245-50.
31. E. E. Underwood: in *Quantitative Stereology*, Addison-Wesley Publishing Co., Reading, MA, 1970, p. 48.
32. C. Carry and J. L. Strudel: *Acta Metall.*, 1977, vol. 25, pp. 767-77.
33. G. R. Leverant, B. H. Kear, and J. M. Oblak: *Metall. Trans.*, 1973, vol. 4, pp. 355-62.
34. S. M. Copley and B. H. Kear: *Trans. AIME*, 1967, vol. 239, pp. 977-84.
35. J. K. Tien and R. P. Gamble: *Metall. Trans.*, 1972, vol. 3, pp. 2157-62.